Enhancing Elevator Ride Quality through Vector Control Techniques and S-Curve Profiles

Ali Abdulkareem Ali
Control & Energy Management Laboratory, Sfax Engineering School, University of Sfax, Sfax, Tunisia
ali-abulkareem.ali@enis.tn (corresponding author)

Fatma Ben Salem
Prince Sattam Bin Abdulaziz University, College of Engineering, Department of Electrical Engineering, Alkharj, 11942, Saudi Arabia
f.bensalem@psau.edu.sa

Jamal A.-K. Mohammed
Electromechanical Engineering Department, University of Technology, Baghdad, Iraq
50128@uotechnology.edu.iq

Received: 10 October 2024 | Revised: 28 October 2024 | Accepted: 30 October 2024

 DOI: https://doi.org/10.48084/etasr.9228

ABSTRACT

This study examines motor drive techniques, including Field-Oriented Control (FOC), sensorless FOC, and Direct Torque Control (DTC), to improve elevator ride quality by reducing jerk-sudden changes in acceleration that cause discomfort. A 200 cm tall prototype elevator system was developed, using S-curve velocity profiles alongside the considered control strategies. The system includes a TMS320F28379D DSP-controlled induction motor, sensors, and an encoder to assess performance. Results show that FOC with S-curve profiles reduces jerk by 72–73%, significantly improving comfort compared to the standard trapezoidal profile. Sensorless FOC reduces jerk by 68–71%, providing a cost-effective option, though it faces challenges during downward motion under load. DTC, reduces jerk by 65–68% and results in less smooth travel, especially during downward movement. In comparison, the trapezoidal velocity profile produced higher jerk levels and less ride comfort. This study emphasizes the critical role of control technique selection in enhancing elevator comfort and efficiency.

Keywords-elevator; jerk reduction; induction motor; elevator systems; Field-Oriented Control (FOC); sensorless FOC; Direct Torque Control (DTC); S-curve profile; Variable-Speed Drives (VSDs); Digital Signal Processor (DSP)

I. INTRODUCTION

Elevators serve as vertical transportation systems for passengers and cargo in both commercial and residential buildings. While the fundamental design of electric elevators has remained consistent since their inception, significant advancements in control systems, safety features, and drive technologies have made modern elevators faster and more reliable and efficient [1]. Today's elevators must offer high transport speeds, precise positioning, minimal jerk, and quick, efficient control with minimal sensor input. Electric elevators, the most commonly used type, are further categorized into traction, linear motor, and drum-driven systems. Among these, traction systems dominate the market due to their effectiveness in high-rise buildings [2]. Passenger comfort and safety are paramount, especially in high-speed elevators that can reach speeds up to 18 m/s. However, such systems often face challenges with vibrations and jerks, particularly during starting and stopping phases, which not only affect ride comfort but also strain mechanical and electrical components [3]. To address these issues, modern research has focused on refining motor control through Variable-Speed Drives (VSDs), aiming to achieve smoother acceleration, minimize jerk, and enhance energy efficiency [4].

Many studies have investigated motor control methods to enhance elevator performance. Initial endeavors, exemplified in [5], implemented electronic control systems using speed feedback to enhance ride comfort and floor-leveling precision. Authors in [6, 7] concentrated on energy-efficient controls and vibration mitigation systems to improve ride quality. Recent studies have investigated the application of artificial

intelligence, fuzzy logic, and sophisticated braking strategies to enhance system performance.

VFDs have been widely adopted in motor performance optimization comparing regenerative and non-regenerative systems [8]. Authors in emphasized the importance of acceleration feedback in suppressing vibrations in induction motor-driven elevators. Authors in [10] further highlighted the need for precise control to balance energy efficiency with ride comfort. Recent studies have focused on reducing jerk in elevators by combining S-curve profiles with control strategies like Direct Torque Control (DTC) and Field-Oriented Control (FOC). Authors in [11, 12] highlight FOC's effectiveness in precise speed control, while authors in [13] achieved an 88% reduction in jerk using an S-curve in a three-story elevator prototype. Additional research [14] on brake control methods further improved deceleration and ride comfort, complementing authors in [15] who developed a stable, cost-efficient control system using SPWM. The development of advanced motor control techniques has been critical in optimizing elevator systems, particularly in reducing jerk to enhance ride comfort.

More studies highlight the advantages of combining control algorithms such as FOC and DTC to achieve superior performance across various torque demands. For instance, in [16], a combined approach of Direct Torque Stator Flux Control (DTSFC) and Direct Torque Rotor Flux Control (DTRFC), paired with FOC, demonstrated excellent torque management, achieving rapid response times and minimal chattering. This foundation supports the exploration of DTC's potential in elevator applications, especially when control smoothness is critical for ride quality. Furthermore, techniques that refine DTC with Space Vector Pulse Width Modulation (SVPWM) and fractional-order sliding mode control have shown reduced torque ripple and enhanced robustness under load variations, providing a basis for achieving stability in dynamic scenarios like elevator motion [17]. These studies underscore the relevance of DTC in elevator systems, where stable, low-ripple control is essential. FOC, widely used in motor control applications, especially benefits from sensorless configurations that eliminate the need for additional position sensors, balancing control accuracy with cost-effectiveness [18]. In elevators, where cost efficiency is often a priority, sensorless FOC offers a practical alternative for maintaining smooth speed transitions without extensive sensor networks. The application of limited-jerk sinusoidal trajectories in FOC systems has shown significant promise in minimizing torque ripple and extending motor life, underscoring the value of smooth trajectory planning [19]. S-curve profiles, which also provide continuous acceleration, are increasingly utilized in elevator systems to address similar challenges, reducing the mechanical strain caused by abrupt motions. Extending this principle, integrating S-curve profiles with DTC algorithms in elevator systems has been shown to reduce jerk by up to 57.2%, improving ride comfort and operational longevity [20].

Despite these advances, there is a need for a comprehensive comparison of FOC, sensorless FOC, and DTC under various load conditions. This study addresses this gap by evaluating these control methods in a prototype elevator system designed to minimize jerk and enhance comfort using S-curve velocity profiles. The system utilizes advanced vector control techniques implemented on Digital Signal Processors (DSPs) to ensure smooth transitions and reduce vibrations, optimizing elevator speed and movement across three floors.

II. JERK ELEVATOR CONTROL

Jerk, defined as the rate of change of acceleration, significantly influences elevator smoothness. Traditional trapezoidal velocity profiles, where acceleration abruptly changes, can cause sudden shocks that adversely affect both mechanical integrity and passenger comfort, reducing positioning accuracy while increasing overshoot and settling time. This leads to mechanical strain and discomfort. Conversely, S-curve profiles, characterized by continuous acceleration curves, smooth these transitions, thereby minimizing these negative impacts. Elevator systems often utilize either triangular or trapezoidal motion profiles. In trapezoidal profiles, the system accelerates to maximum speed, maintains it, then decelerates. Triangular profiles, on the other hand, accelerate directly to peak speed and then decelerate immediately, without maintaining a constant speed. Both profiles, however, lead to abrupt velocity changes, generating jerk and resulting in vibrations and passenger discomfort.

To alleviate these issues, motion control systems increasingly implement S-curve profiles, which smooth acceleration and deceleration phases, effectively reducing jerk and enhancing ride comfort and system precision. Based on the methodology in [20], the equations for S-curve jerk control are directly applied as follows:

$$a = \begin{cases} \frac{j_m T\left(1-cos\left(\frac{2\pi}{T}t\right)\right)}{2\pi}, \\ a_m \ , \\ -\frac{j_m T\left(1+cos\left(\frac{2\pi}{T}(t_2-t)\right)\right)}{2\pi} \end{cases} \quad (1)$$

$$v = \begin{cases} \frac{j_m T\left(2\pi t - T\,sin\left(\frac{2\pi}{T}t\right)\right)}{4\pi^2} \\ \frac{j_m T^2}{2\pi} \\ \frac{j_m T}{2\pi}\left(T - \frac{\left(T\,sin\left(\frac{2\pi}{T}(t_2-t)\right)+2\pi(t-t_2)\right)}{2\pi}\right) \end{cases} \quad (2)$$

$$d = \begin{cases} \frac{j_m T}{4\pi}\left(t^2 - \frac{T^2\left(1-cos\left(\frac{2\pi}{T}t\right)\right)}{2\pi^2}\right), & t \in [0, T] \\ \frac{j_m T^2}{4\pi}(2t - T), & t \in [T, t_2] \\ \frac{j_m T^2}{4\pi}\left[(2t-T) - \frac{(t-t_2)^2}{T} + \frac{T}{2\pi^2}\left[1 - cos\frac{2\pi}{T}(t-t_2)\right]\right], & t \in [t_2, t_3] \end{cases} \quad (3)$$

In this context, t_3 represents the total duration of cabin movement, T denotes the time allocated for acceleration or deceleration, t_2 is defined as t_3 - T, marking the moment when the cabin initiates deceleration, and j_m signifies the maximum amplitude of jerk. Figure 1 shows the comparison between the trapezoidal, triangular and S-curve velocity profiles.

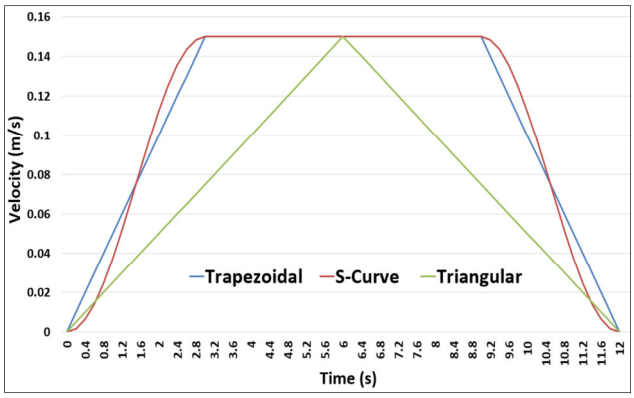

Fig. 1. Comparison of trapezoidal and S-curve velocity profiles.

III. EXPERIMENTAL WORK

This study presents a prototype elevator system designed to simulate a full-scale elevator, incorporating advanced controls for enhanced ride comfort and safety. Constructed from durable iron, the structure spans three levels and measures 200 × 45 × 55 cm, offering a stable and compact framework suitable for experimentation. The elevator car, a key component in this inter-floor transportation system, is made from aluminum, chosen for its excellent strength-to-weight ratio. The car measures 19 × 30 cm and can handle a total load of 23.3 kg, including its own mass, mimicking real elevator load conditions. The system employs two 7 cm diameter pulleys to enable the vertical movement of the elevator car. These pulleys, connected by cables to the car, ensure smooth, balanced travel both upwards and downwards with minimal friction or mechanical resistance, as shown in Figure 2. A double pulley setup minimizes lateral sway during operation, contributing to the safety and comfort of the elevator's movement.

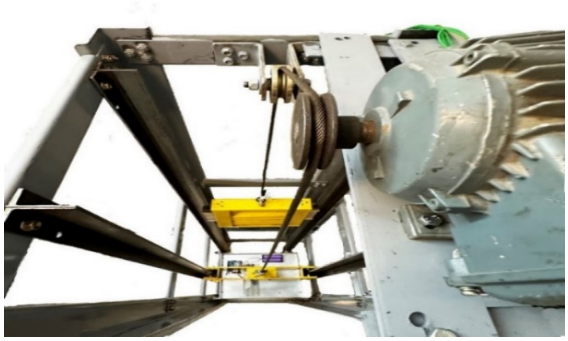

Fig. 2. The elevator pulleys.

The system uses a 0.75 kW, 3-phase Induction Motor (IM) in a Y-connection, operating at 1395 rpm and 460 V / 50 Hz, with a power factor of 0.75. This motor, delivering 8 Nm of torque and drawing a line current of 2 A, efficiently raises and lowers the elevator car, including its load, across three floors. It features a braking mechanism for secure stops during loading, unloading, or emergencies, enhancing safety. Additionally, a counterweight opposite the elevator car balances the load, reducing motor strain and improving energy efficiency, thus extending component longevity and ensuring a reliable elevator system. The elevator is equipped with four buttons—three for floor selection and one for emergencies.

A. Digital Signal Processing

Texas Instruments' TMS320F28379x microcontrollers, a part of the C2000™ family, are ideal for demanding industrial and automotive applications. These microcontrollers are particularly effective in motor drive control, power conversion, and automation. They feature high-resolution PWM modules and fast ADCs for precise control and monitoring of electrical variables in motor drives. Development is supported by tools such as Code Composer Studio (CCS), C2000Ware, and MATLAB/Simulink, enhancing efficiency in high-performance motor control and power conversion applications. The integration of motor drives is further streamlined by the LAUNCHXL-F28379D Dock Station Board, which enhances system flexibility and performance, as illustrated in Figure 3.

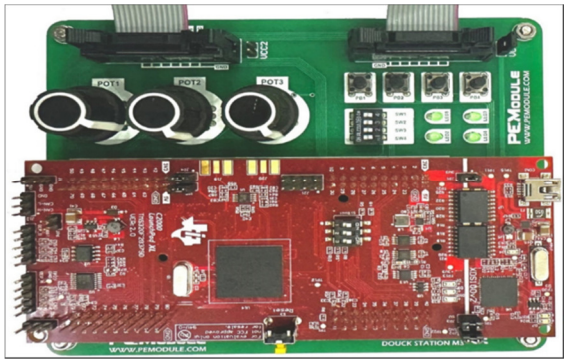

Fig. 3. TMS320F28379x and dock station board.

B. Current and Voltage Transducers

Differential transducers in this system provide complete isolation while measuring current and voltage, ensuring the safe and efficient functioning of motor drives. The current transducer utilizes opto-isolation to accurately measure true RMS current across both AC and DC waveforms. It features a bandwidth of 200 kHz, linearity of 0.5%, and gain accuracy of ±1%, along with 3 kV isolation to handle high-interference environments. Similarly, the voltage transducer delivers precise AC/DC voltage measurements with the same bandwidth and linearity, and is equipped to manage high-voltage scenarios with 15 kV/s transient immunity and 3 kV isolation.

Both transducers are integrated into the system's Three Module Power Electronics Base Board, as depicted in Figure 4, which handles up to 800V/20A. Their outputs, which are refined and stabilized, connect to the DSP's ADC inputs for reliable, noise-free operation. Isolation components protect the DSP, while precisely calibrated DSP firmware ensures accurate motor control, enhancing both safety and performance critical for smooth elevator operations.

C. Jerk Mesurment

An MPU6050 accelerometer sensor was used with an Arduino Uno R4 WiFi to measure jerk in an elevator system. The Arduino Uno R4 combines the simplicity of the original

Arduino with wireless capabilities, facilitating real-time data collection and remote integration for applications like home automation. The MPU6050 sensor, which includes a 3-axis gyroscope and a 3-axis accelerometer with an integrated Digital Motion Processor (DMP), analyzes motion data effectively. It provides adjustable sensitivity ranges, from ±250 to ±2000 degrees per second for the gyroscope, and ±2g to ±16g for the accelerometer. The MPU6050 accelerometer records real-time acceleration data along the elevator's axis at a set sampling frequency. Using these acceleration values, jerk is calculated as the rate of change of acceleration with respect to time by taking finite differences between successive measurements. This method allows for precise jerk analysis during acceleration and deceleration, providing insight into motion smoothness. Integrated into an elevator car, the Arduino Uno R4 WiFi and a compact onboard power supply collect real-time acceleration and jerk data, crucial for assessing elevator performance. The use of WiFi eliminates the need for extensive wiring, simplifying data transmission as illustrated in Figure 5. An external battery enhances mobility and ensures continuous operation, ideal for elevator settings.

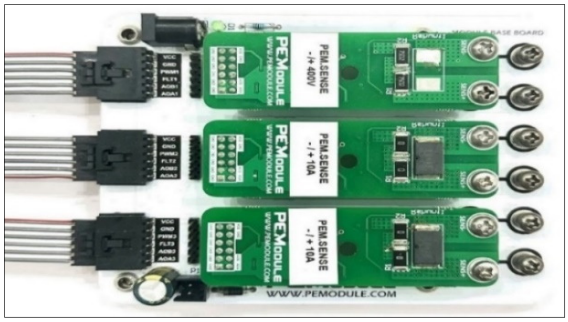

Fig. 4. The board with current and voltage transducers.

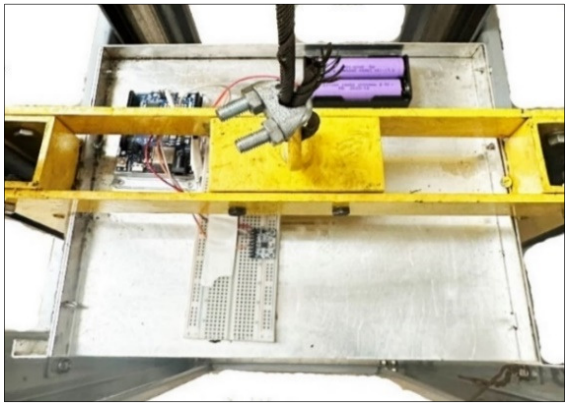

Fig. 5. The system of jerk sensor.

D. Inverter

The inverter is essential for transforming DC voltage into AC power to operate a three-phase induction motor. It employs six IGBTs (Insulated Gate Bipolar Transistors) that swiftly toggle the DC voltage, producing the necessary AC waveform for motor function. The IGBT module, with an integrated forward diode, is engineered for high-performance applications, accommodating up to 1200V and 50A. It encompasses features such as temperature regulation and a gate driver for improved efficiency, with a low saturation voltage to minimize switching losses. The DSP generates PWM signals to control the IGBTs, determining the timing for AC waveform generation. The inverter receives DC inputs from a rectified power source or battery and outputs three AC phases (U, V, W) to the motor. A pair of capacitors stabilizes the DC input to ensure consistent AC waveform generation and smooth motor performance, as shown in Figure 6.

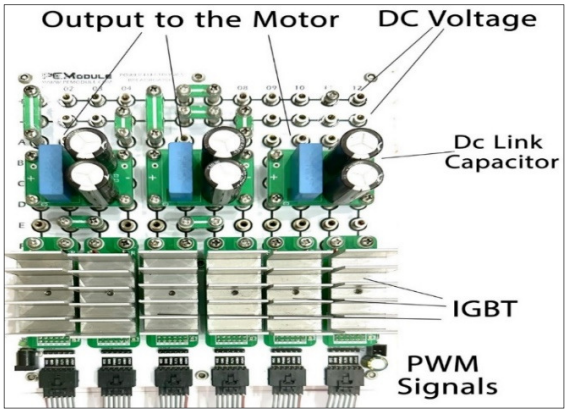

Fig. 6. The inverter.

The Six Modules Signal Collector Board, depicted in Figure 7, supports up to 800V/20A and streamlines connections to signal conditioning circuits. It includes a single connector for all PWM control signals and another for analog signals, significantly simplifying wiring. Additionally, test points for both PWM and analog signals are available, facilitating easier testing and troubleshooting.

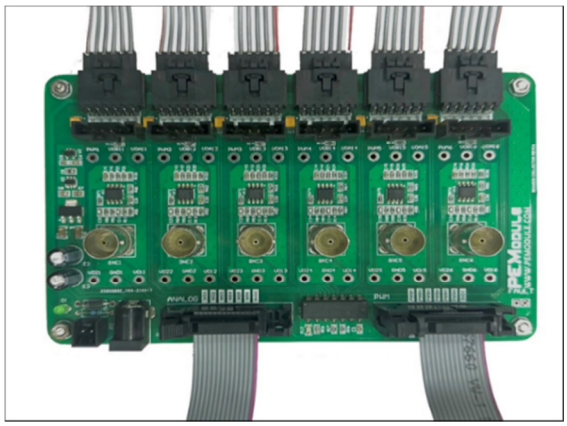

Fig. 7. The six module signal collector board.

Figure 8 shows the prototype elevator, consisting of a metal frame structure with a pulley system driven by a motor mounted at the top. This setup demonstrates an elevator mechanism for experimentation and testing purposes.

Fig. 8. The prototype elevator.

IV. RESULTS

This section evaluates the practical performance of FOC, sensorless FOC, and DTC in elevator systems, providing insights into how each method minimizes jerk and enhances ride smoothness. Experimental data underline the effectiveness of these control strategies. The DSP produces PWM signals through channels 1, 2, and 3, with complementary signals A and B. These signals ensure that one transistor is active while the other is inactive, optimizing motor control and preventing short circuits. A chosen frequency of 10 kHz improves control efficiency by minimizing switching losses and noise.

The DSP modulates the PWM signals' duty cycle to precisely control the motor's speed and torque. These signals drive the IGBTs in the inverter, converting DC power into three-phase AC, crucial for the motor's operation. Accurate generation and timing of PWM signals are vital for ensuring smooth motor control and efficient operation of the elevator system. This study used a trapezoidal velocity profile with a maximum speed of 0.15 m/s as the baseline for comparison before introducing the S-curve profile. Figure 9 displays the encoder measurements, while Figure 10 shows the jerk profile associated with the trapezoidal velocity profile. Figure 11 shows the applied S-Curve velocity profile.

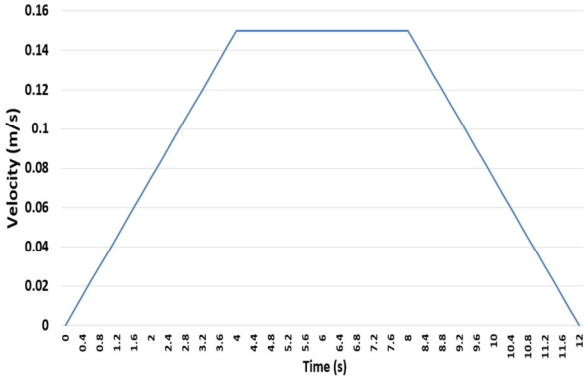

Fig. 9. Trapezoidal velocity profile.

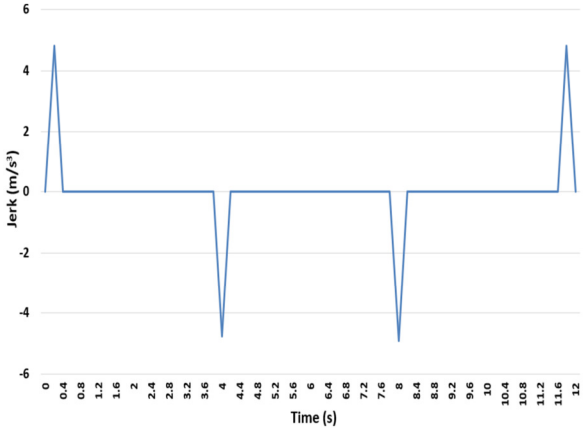

Fig. 10. Jerk profile with trapezoidal profile.

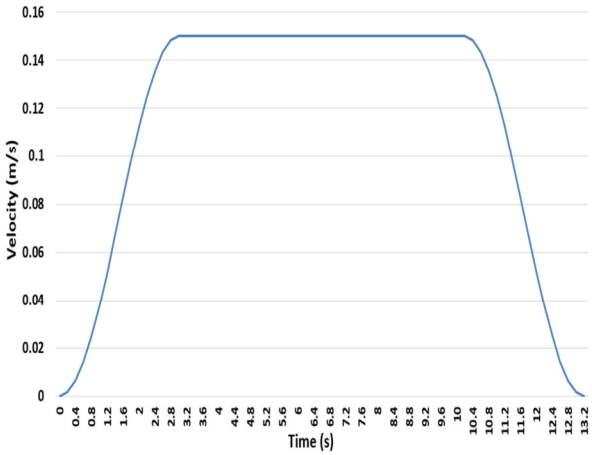

Fig. 11. S-curve velocity profile.

Figure 12 encapsulates the jerk profiles for DTC, FOC, and sensorless FOC, under loaded conditions, highlighting their respective challenges and performance. DTC faces difficulty during loaded upward movement, with jerk values reaching 1.55 m/s³, indicating abrupt transitions that compromise ride comfort. Conversely, sensorless FOC shows more controlled behavior with jerk values of 1.38 m/s³ in both upward and downward movements, suggesting it manages the load adequately despite lacking direct sensor feedback, which

results in slightly rougher transitions. Additionally, standard FOC, while loaded, demonstrates effective jerk control with values of 1.28 m/s³ and -1.274 m/s³ during upward movements.

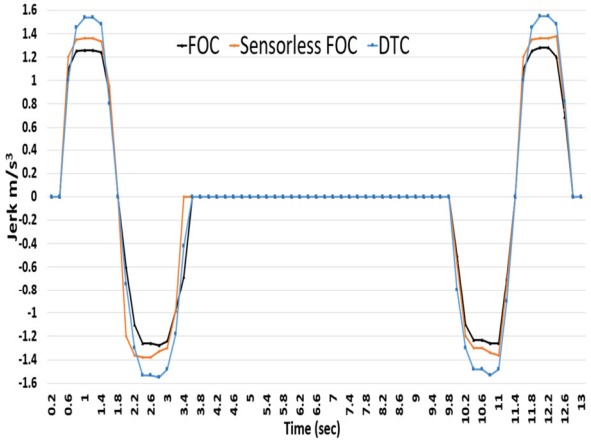

Fig. 12. Jerk profiles in loaded upward motion.

The comparison of Figures 10 and 12 underscores the S-curve's ability to reduce peak jerk values, with FOC achieving the smoothest profile, sensorless FOC offering a balanced, cost-effective alternative, and DTC exhibiting slightly higher jerk levels under loaded conditions. The S-curve profile effectively reduces both the intensity and frequency of jerk peaks, enhancing ride comfort and meeting industry standards.

Figure 13 illustrates the challenges of DTC during loaded downward movements, where jerk peaks at 1.53 m/s³ positively and -1.51 m/s³ negatively, suggesting that gravitational pull and load exacerbate deceleration challenges and hinder smooth transitions. Similarly, sensorless FOC faces difficulties with a positive jerk of 1.43 m/s³ and a negative of 1.45 m/s³, struggling to achieve smooth deceleration due to the lack of direct feedback and compounded external forces. Standard FOC, however, shows a smaller increase in jerk, with 1.28 m/s³ positive and -1.294 m/s³ negative, managing to maintain smoother operations under the same conditions. This analysis highlights the varying performance of these control strategies in managing jerk, particularly during downward movements under load.

Comparing the jerk time between Figures 10, 12, and 13, the trapezoidal velocity profile in Figure 10 exhibits higher peak jerk levels with more abrupt changes, leading to shorter but intense periods of jerk during the acceleration and deceleration phases. This concentrated jerk time results in sudden transitions that increase discomfort. Conversely, Figures 12 and 13 show that the S-curve profile distributes jerk over a longer period, especially during acceleration and deceleration, resulting in smoother transitions with extended, but lower-intensity jerk phases. By spreading the jerk time, the S-curve profile reduces peak jerk, improving comfort and reducing mechanical strain. The jerk time in S-curve profiles extends across both acceleration and deceleration, smoothing out motion changes and aligning with ISO standards for elevator jerk limits.

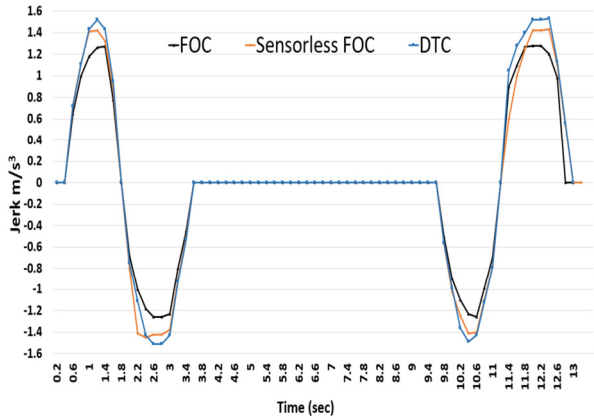

Fig. 13. Jerk profiles in loaded downward motion.

The same process was conducted under no-load conditions, yielding results similar to those with load. The results demonstrate that FOC with S-curve profiles effectively reduces jerk by 72–73%, significantly enhancing comfort over the standard trapezoidal profile. Sensorless FOC achieves a jerk reduction of 68–71%, offering a cost-effective alternative, albeit with performance challenges during loaded downward motion. DTC also reduces jerk by 65–68%.

Figure 14 demonstrates the percentage of jerk reduction achieved by DTC, Sensorless FOC, and FOC in various load scenarios using the S-curve profile compared to the trapezoidal profile.

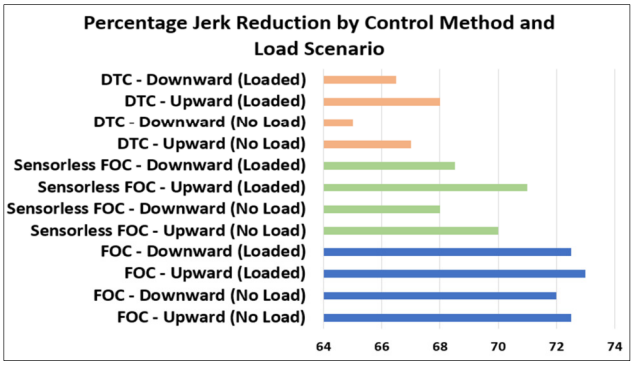

Fig. 14. Jerk reduction **p**ercentage.

V. CONCLUSIONS

This study evaluated three vector control methods—FOC, sensorless FOC, and DTC—for minimizing jerk and improving ride comfort in elevator systems, specifically using S-curve velocity profiles. Compared to prior work such as [20], which evaluated only DTC with S-curve and achieved a jerk reduction of approximately 57.2%, this study uniquely contributes by analyzing the strengths and limitations of FOC, sensorless FOC, and DTC under varying load conditions. Results demonstrate that FOC with S-curve profiles achieves a jerk reduction of 72–73% over traditional trapezoidal profiles, representing a significant improvement of 15–16% in jerk reduction. Sensorless FOC reduces jerk by 68–71%, while DTC shows a reduction of 65–68%, with FOC consistently

providing the best performance. This insight enables practitioners to make informed choices in control methods based on specific performance requirements and cost considerations.

The findings also highlight that both the direction of movement and load conditions significantly impact jerk performance. Upward movements generally show better jerk reduction due to more effective compensation for gravitational forces. According to ISO 8100-34:2021, elevator jerk should not exceed 1.2 m/s³. The results indicate that FOC with S-curve profiles meets this standard, thereby enhancing both comfort and compliance.

Future research can explore further enhancements to FOC by integrating advanced sensor technologies to improve accuracy, refining sensorless FOC algorithms to bridge the gap with FOC, and optimizing DTC for smoother transitions and better jerk control. Additionally, adaptive S-curve profiles could be developed to dynamically adjust ride comfort in real-time, while accounting for external factors such as temperature and load distribution to refine control strategies even further.

In conclusion, FOC remains the most reliable method for minimizing jerk and ensuring smooth elevator operation under varying conditions, but continued research in these areas could lead to even greater improvements in system performance and passenger comfort.

REFERENCES

[1] K. Al-Kodmany, "Elevator Technology Improvements: A Snapshot," *Encyclopedia*, vol. 3, no. 2, pp. 530–548, Jun. 2023, https://doi.org/10.3390/encyclopedia3020038.

[2] G. Zhang, G. Wang, N. Zhao, and D. Xu, *Permanent Magnet Synchronous Motor Drives for Gearless Traction Elevators*. New York, NY, USA: Springer, 2022.

[3] D. Hu, Q. Wang, and J. Zhan, "Research on Vibration Reduction Characteristics of High-Speed Elevator with Rolling Guide Shoes Based on Hydraulic Damping Actuator," *Actuators*, vol. 13, no. 9, Sep. 2024, Art. no. 356, https://doi.org/10.3390/act13090356.

[4] M. Zhao, C. Qin, R. Tang, J. Tao, S. Xu, and C. Liu, "An Acceleration Feedback-Based Active Control Method for High-Speed Elevator Horizontal Vibration," *Journal of Vibration Engineering & Technologies*, vol. 12, no. 2, pp. 1943–1956, Feb. 2024, https://doi.org/10.1007/s42417-023-00955-z.

[5] K. Rajaraman and S. K. Nagaraja, "An Elevator Speed-Control System Using Squirrel-Cage Induction Motors," *IEEE Transactions on Industrial Electronics*, vol. IE-31, no. 2, pp. 164–167, Feb. 1984, https://doi.org/10.1109/TIE.1984.350063.

[6] N. Mutoh, N. Ohnuma, A. Omiya, and M. Konya, "A motor driving controller suitable for elevators," *IEEE Transactions on Power Electronics*, vol. 13, no. 6, pp. 1123–1134, Aug. 1998, https://doi.org/10.1109/63.728339.

[7] Y.-M. Lee, J.-K. Kang, and S.-K. Sul, "Acceleration feedback control strategy for improving riding quality of elevator system," in *Conference Record of the 1999 IEEE Industry Applications Conference. Thirty-Forth IAS Annual Meeting (Cat. No.99CH36370)*, Phoenix, AZ, USA, Oct. 1999, vol. 2, pp. 1375–1379, https://doi.org/10.1109/IAS.1999.801680.

[8] A. B. Kulkarni, H. Nguyen, and E. W. Gaudet, "A comparative evaluation of fine regenerative and nonregenerative vector controlled drives for AC gearless elevators," in *Conference Record of the 2000 IEEE Industry Applications Conference. Thirty-Fifth IAS Annual Meeting and World Conference on Industrial Applications of Electrical Energy (Cat. No.00CH37129)*, Rome, Italy, Oct. 2000, vol. 3, pp. 1431–1437, https://doi.org/10.1109/IAS.2000.882072.

[9] J.-K. Kang and S.-K. Sul, "Vertical-vibration control of elevator using estimated car acceleration feedback compensation," *IEEE Transactions on Industrial Electronics*, vol. 47, no. 1, pp. 91–99, Oct. 2000, https://doi.org/10.1109/41.824130.

[10] L. Al-Sharif, "Variable Speed Drives in Lift Systems," *Elevator World*, vol. 49, pp. 96–106, Sep. 2001.

[11] S. Rangarajan and V. Agarwal, "Load Sensorless Novel Control Scheme for Minimizing the Starting Jerk and Energy of the PMSM Driven Gearless Elevators With Varying Stiction and Rotor Flux Linkage," in *IEEE Transportation Electrification Conference (ITEC-India)*, Bengaluru, India, Dec. 2019, pp. 1–6, https://doi.org/10.1109/ITEC-India48457.2019.ITECINDIA2019-225.

[12] A. So and W. L. Chan, "Comprehensive model of linear PMSM-based ropeless lift for comparing control algorithms – Field-oriented control versus direct torque control," *Building Services Engineering Research and Technology*, vol. 41, no. 6, pp. 659–680, Nov. 2020, https://doi.org/10.1177/0143624419899058.

[13] S. A. Othman, J. A.-K. Mohammed, and F. M. Mohammed, "Implementation of linear elevator with high riding quality based on Scurve profile," *AIP Conference Proceedings*, vol. 2415, no. 1, Dec. 2022, Art. no. 030009, https://doi.org/10.1063/5.0092879.

[14] T. Duong and V. Nguyen, "Improves the Brake Working of the Rescue Winch to Control the Stop Brake Process," *Advances in Science and Technology Research Journal*, vol. 18, no. 1, pp. 255–267, Feb. 2024, https://doi.org/10.12913/22998624/177662.

[15] H. Qin, "Elevator Drive Control system based on single Chip Microcomputer," in *8th International Conference on Mechatronics, Computer and Education Informationization*, Shenyang, China, Dec. 2018, pp. 137–143, https://doi.org/10.2991/mcei-18.2018.27.

[16] M. Elgbaily, F. Anayi, and M. M. Alshbib, "A Combined Control Scheme of Direct Torque Control and Field-Oriented Control Algorithms for Three-Phase Induction Motor: Experimental Validation," *Mathematics*, vol. 10, no. 20, Jan. 2022, Art. no. 3842, https://doi.org/10.3390/math10203842.

[17] S. K. Gudey, M. Malla, K. Jasthi, and S. R. Gampa, "Direct Torque Control of an Induction Motor Using Fractional-Order Sliding Mode Control Technique for Quick Response and Reduced Torque Ripple," *World Electric Vehicle Journal*, vol. 14, no. 6, Jun. 2023, Art. no. 137, https://doi.org/10.3390/wevj14060137.

[18] S. Rajinth, C. Abeykoon, and D. H. S. Maithripala, "Design of a Sensorless Field Oriented Control Drive for Brushless DC Motors," in *9th International Conference of Control, Dynamic Systems, and Robotics*, Niagara Falls, Canada, Jun. 2022, pp. 1–9, https://doi.org/10.11159/cdsr22.180.

[19] M. K. Mutlu, "Limited-jerk sinusoidal trajectory design for field oriented control of permanent magnet synchronous motors with H-infinity optimal controller," M.S. thesis, Middle East Technical University, Cankaya, Ankara, Turkey, 2019.

[20] A. A. Ali, F. B. Salem, and J. A.-K. Mohammed, "Design of an Electric Elevator Drive with High Riding Quality under Jerk Control," *Engineering, Technology & Applied Science Research*, vol. 14, no. 5, pp. 16438–16443, Oct. 2024, https://doi.org/10.48084/etasr.8202.